This article has been accepted for publication in a future issue of this journal, but has not been fully edited. Content may change prior to final publication. Citation information: DOI 10.1109/LPT.2014.2311454, IEEE Photonics Technology Letters

Corrugated Waveguide Based Optical Phased Array with Crosstalk Suppression

David Kwong, Amir Hosseini, John Covey, Xiaochuan Xu, Yang Zhang, Swapnajit Chakravarty, and Ray T. Chen, *Fellow, IEEE*

***Abstract*— We present the corrugated waveguide as a free space grating coupler for use in optical phased arrays for large angle optical beam steering. Compared to conventional shallow etched gratings, the corrugated waveguide requires only a single patterning step while achieving lithographically defined index contrast. We achieve 15° of steering with wavelength tuning, with an average longitudinal beam width of 0.3°. To prevent optical crosstalk from grating assisted coupling in a corrugated waveguide array with small element spacing, the photonic bandgap of a 2D photonic crystal is used to optically isolate each array element in a 16 element array.**

***Index Terms*—Optical waveguide, photonic integrated circuit, silicon nanomembrane, phased array, gratings, photonic crystal**

I. Introduction

Optical phased arrays (OPAs) integrated on chip can provide agile and precise beam steering in free space without any mechanical parts. They can be used for a variety of beam steering applications, including LIDAR and other mapping applications, or point-to-point communications in metropolitan regions or high performance computing systems. Recent optical phased arrays fabricated on silicon on insulator (SOI) achieve free space optical beam steering through wavelength tuning of shallow etched gratings, which reduces a silicon grating's inherently large index contrast in order to decrease the grating strength [1,2]. This increases the effective aperture of the emitted optical signal, and ultimately results in narrow far field beam widths. However, shallow etched gratings not only require precise etching control, but the multiple patterning steps that are required also increase fabrication complexity and cost. Acoleyen et al. achieved a beam width of ~2.5° by shallow etching 70nm of the 220nm silicon device layer [1]. Doylend et al. used a significantly thicker silicon layer of 500nm and shallow etched the output gratings by 75nm to achieve a beam width of 0.6° [2]. While using a thicker silicon layer can reduce the index contrast for a given etch depth, the disadvantage of this approach is the higher power consumption required to achieve thermo-optic phase shifting due to heating an increased waveguide volume.

This research is supported by the Multi-disciplinary University Research Initiative (MURI) program through AFSOR, Contract #FA 9550-08-1-0394.

D. Kwong, J. Covey, X. Xu, Y. Zhang, and R. T. Chen are with the University of Texas at Austin, Austin, TX 78758 (email: diddykwong@gmail.com;john.yevoc@gmail.com; xiaochuan.xu@utexas.edu; magicloudy@gmail.com; raychen@uts.cc.utexas.edu);

A. Hosseini and S. Chakravarty are with Omega Optics, Inc., Austin, TX, 78759 (email:amirh@utexas.edu; swapnajit.chakravarty@omegaoptics.com)

In addition, due to the thickness of the silicon layer, which supports multiple vertical modes, rib waveguides are needed for single mode propagation, thereby adding an additional patterning step. It is desirable to utilize a structure that requires only a single patterning step, and can also realize small index contrasts necessary for achieving narrow longitudinal beamwidths, while still using single mode silicon device layers.

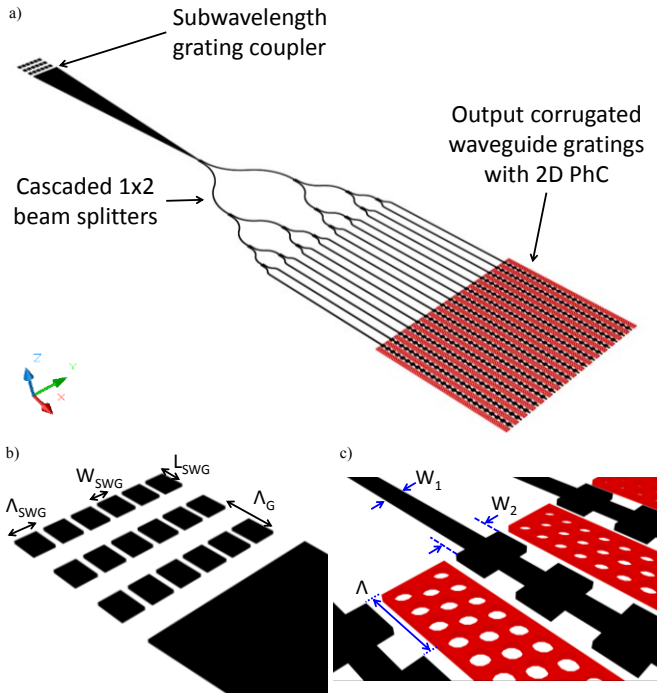

Fig. 1-(a) Schematic of the grating coupled 16 element optical phased array consisting of corrugated waveguides separated by 2D PC. (b) Closeup view of the subwavelength grating coupler. (c) Closeup of the corrugated waveguides with 2D PC isolation.

In this work we present a 16 element OPA fabricated on SOI with a 250nm silicon device layer that uses laterally corrugated waveguides for free space coupling and realizes narrow far field beam widths. Furthermore, we also place 2D photonic crystal (PC) slabs between the array elements for optical crosstalk suppression.

II. Design

A schematic of the OPA is shown in Figure 1(a) and consists of several key components as follows: a wideband subwavelength fiber to waveguide grating coupler for coupling light into the photonic circuit, cascaded 1x2

This article has been accepted for publication in a future issue of this journal, but has not been fully edited. Content may change prior to final publication. Citation information: DOI 10.1109/LPT.2014.2311454, IEEE Photonics Technology Letters

multimode interference (MMI) couplers for optical beam splitting, and the output corrugated waveguide gratings which emit to free space. All of these components are designed for Transverse-Electric (TE) polarization.

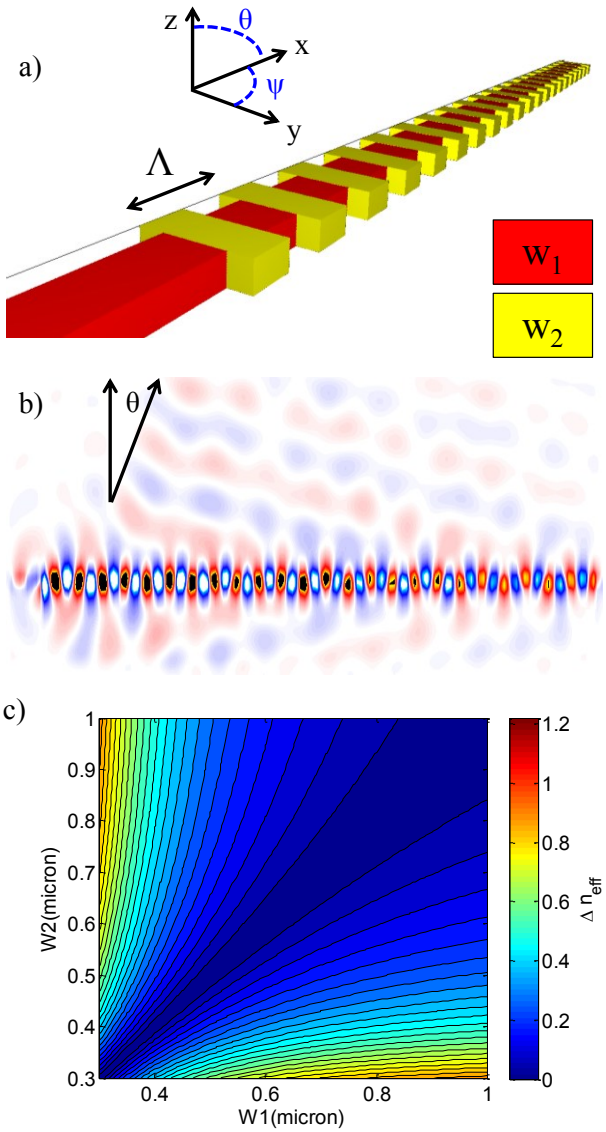

Fig. 2-(a) Schematic of a single corrugated waveguide with period Λ and widths w_1 and w_2. (b) Ex field profile of a corrugated waveguide emission from a 3D FDTD simulation. (c) Contour plot of the differences in effective index between different values of w_1 and w_2 for the fundamental TE mode.

Grating couplers provide advantages in larger misalignment tolerances compared to direct butt coupling or using lensed fibers while eliminating the need for facet preparation. Grating couplers using periodic subwavelength nanostructures (SWN) allow refractive index engineering to increase single mode fiber coupling efficiency while allowing single step patterning [3, 4]. A schematic of the grating coupler with SWN is shown in Figure 1(b). The SWN can be treated as a homogeneous medium according to the effective medium theory (EMT) when the subwavelength period Λ_{SWG} is below the wavelength in the material. From EMT theory, the refractive index of the SWN region n_{SWG} is an intermediate value between a high index material ($n_{high}=n_{si}=3.48$) and low index material ($n_{low}=n_{air}=1$), and is a function of the fill factor, which is defined as W_{SWG}/Λ_{SWG} [3-5].

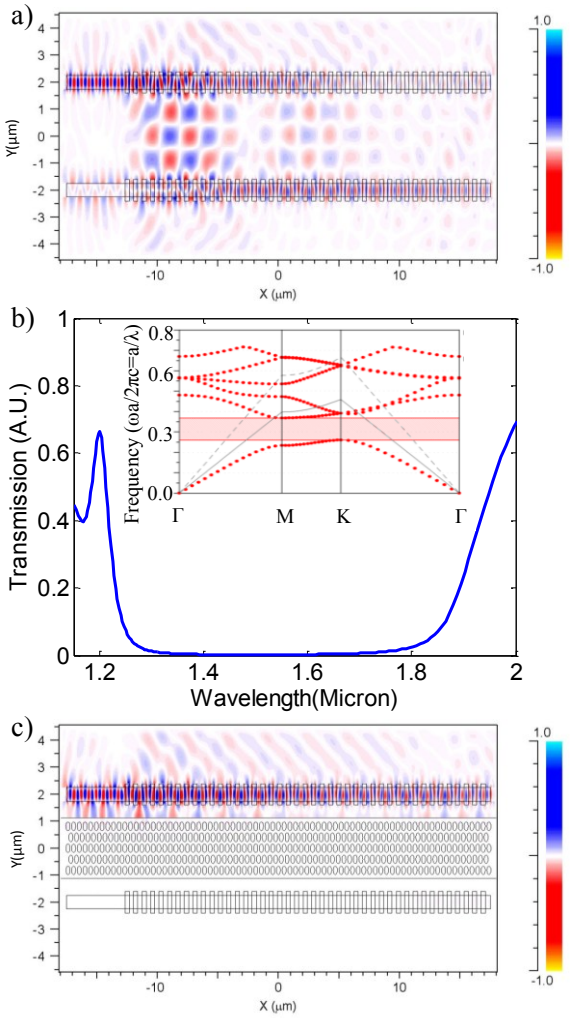

Fig. 3-(a) 2D FDTD simulation of 2 corrugated waveguides spaced 4μm apart showing optical crosstalk between the excited waveguide on top and the waveguide on bottom via grating assisted coupling. (b) Transmission spectrum of a plane wave through 5 periods of the 2D PC slab, with inset showing the band diagram. (c) 2D FDTD simulation of the same structure but with 5 periods of 2D PC between the two corrugated waveguides showing effective crosstalk suppression.

Typical demonstrated silicon based grating couplers have 3dB bandwidths of ~50nm, but our wavelength tuning range of 1480-1580nm necessitates grating couplers with larger bandwidth for wideband operation. By lowering the average effective index of the grating to reduce waveguide dispersion, one can increase the bandwidth [6]. The average effective index of the grating can be lowered by choosing the high index region of the grating as the subwavelength region, and the low index region as the cladding. Using 2D Finite Difference Time Domain (FDTD) simulations, we optimize the grating coupler to arrive at a design of grating period $\Lambda_G=1.3\mu m$ with $L_{SWG}=728nm$ and $n_{swg}=2.15$. We then use EMT theory to choose the subwavelength period $\Lambda_{SWG}=360nm$ with $W_{SWG}=290nm$.

The input light is split into 16 uniform outputs by 4 levels of cascaded 1x2 MMI couplers, which allow for equal output phase profiles due to the symmetry of the structure. These 16

This article has been accepted for publication in a future issue of this journal, but has not been fully edited. Content may change prior to final publication. Citation information: DOI 10.1109/LPT.2014.2311454, IEEE Photonics Technology Letters

outputs are then fed into the 16 element array composed of corrugated waveguides with 4µm spacing.

Laterally corrugated waveguides are essentially alternating waveguide sections with widths w_1 and w_2 periodically repeated by Λ, as shown in Figure 2(a). These corrugations can be fabricated in a single patterning step and allow the structure to function as a free space grating coupler, as shown in the cross sectional E_x field profile of the 3D FDTD simulation in Figure 2(b). The emission angle θ is governed by the phase matching condition [6], and is given by $\sin(\theta) = \left(n_{eff,avg} \times \Lambda - \lambda\right) / \Lambda \times n_{clad}$, where $n_{eff,avg}$ is the average effective index of the two corrugations, Λ is the grating period, λ is the free space wavelength, and n_{clad} is the refractive index of the cladding material. In addition, as the index contrast in the grating is controlled lithographically by the widths w_1 and w_2, very small index contrast can be precisely achieved by properly choosing the desired combination of w_1 and w_2, as seen in Figure 2(c). In our design, w_1=500nm, and w_2=600nm, and Λ=700nm, and there are 430 periods for a total grating length of 301µm, which is sufficient for all of the light to be emitted from the grating. This increased grating length results in a larger emission aperture and provides for narrower longitudinal beam widths.

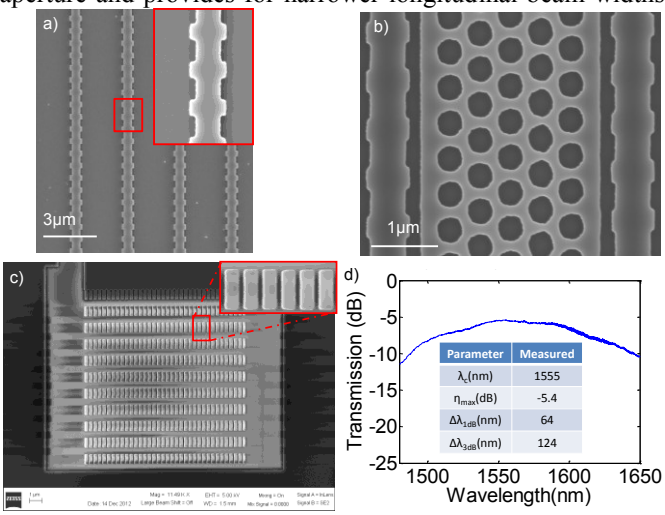

Fig. 4- Top down SEM of the corrugated waveguide OPA (a) without and (b) with the 2D PC in between array elements. (c) Top down SEM of the input subwavelength grating coupler and (d) the input grating's transmission spectrum.

However, these lateral corrugations result in grating assisted coupling between adjacent waveguides [7], which results in optical cross talk between adjacent elements in the OPA and ultimately jeopardizes the far field pattern [8].

This optical crosstalk can be seen in the 2D FDTD simulation of Figure 3(a) where a single corrugated waveguide is excited and light is coupled via the corrugations to the adjacent waveguide 4µm away. This coupling between waveguides limits the minimum element spacing, but for large angle beam steering in OPAs, element spacings on the order of the emission wavelength are required. Thus, inter-element isolation is necessary to maximize the steering angle. In this work, 5 periods of 2D PC are placed between adjacent array elements to prevent inter-element cross talk. The PC consists of a triangular lattice of air holes with a lattice constant *a*=612nm, a radius *r*=0.43*a*, and a photonic bandgap that covers 1300 to 1800nm, which is adequate for the 1480-1580nm range needed for our application. The transmission spectrum of a plane wave through 5 periods of this PC in the XY plane is shown in Figure 3(b) and clearly shows low transmission in the wavelength region of interest. Figure 3(c) shows the same 2D FDTD crosstalk simulation but with 5 periods of PC placed between the two waveguides. It can clearly be seen that the 2D PC effectively suppresses the crosstalk between the waveguides. We note that using 2D FDTD cannot quantify the crosstalk and its reduction using the PC, but rather it is used to qualitatively show the concept of crosstalk reduction between adjacent array elements using 2D PC. We also note that the PC successfully suppresses the grating assisted coupling only for laterally radiated photons. We demonstrate this crosstalk suppression scheme by fabricating a 16 element OPA and comparing it with an identical structure except without PC.

III. CHARACTERIZATION

The device is fabricated on SOI with a top silicon layer of 250nm and 3µm Buried Oxide (BOX). The photonic circuit is patterned in a single step by electron beam lithography and reactive ion etching (RIE). Top down SEMs of the corrugated waveguide without and with 2D PC are shown in Figure 4(a) and (b), respectively, while the SEM of the fiber to waveguide wideband input grating coupler is shown in Figure 4(c).

TE polarized light from a polarization maintaining fiber (PMF) is coupled into the input grating coupler. The input grating coupler is characterized using a separate structure consisting of identical gratings connected by straight waveguide. Assuming equal coupling efficiencies for the input and output grating, the coupling efficiency of a single coupler can be extracted. The transmission spectrum of the input grating coupler is shown in Figure 4(d) and provides a 3dB bandwidth of 124nm with a maximum coupling efficiency η_{max}=-5.4dB at a central wavelength of λ_c=1555nm, which is sufficient to fully cover our wavelength tuning range. The far field pattern is directly observed on an IR CCD that is suspended above the device.

We first observe the far field pattern of a single corrugated waveguide, which forms the steering envelope for the array. By tuning the wavelength in 10nm steps, we observe the expected steering of the far fields as shown in the IR images in Figure 5(a). The beam profiles in the longitudinal direction θ (XZ plane) are shown in Figure 5(b), and the steering angle with the Full Width Half Maximum (FWHM) beam widths are shown in Figure 5(c). It can be seen that the average beam width in this steering range is ~0.3°.

The two OPAs with and without the 2D PC isolators were then tested. Figure 6(a) shows the far field pattern of the 16 element OPA with 4 micron spacing without any 2D PC in between. Multiple bands in the far field

This article has been accepted for publication in a future issue of this journal, but has not been fully edited. Content may change prior to final publication. Citation information: DOI 10.1109/LPT.2014.2311454, IEEE Photonics Technology Letters

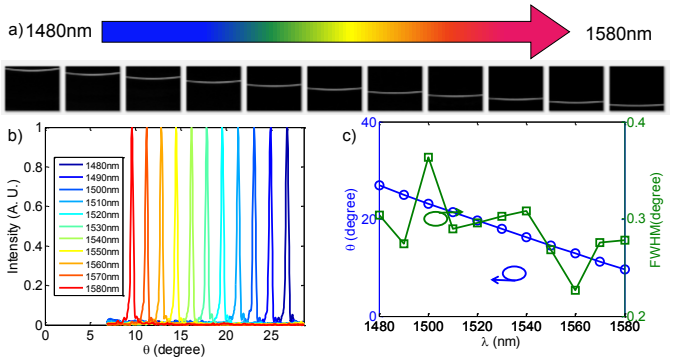

Fig. 5-(a) IR CCD image of the far field of a single corrugated waveguide as the wavelength is tuned from 1480nm to 1580nm in 10nm steps. (b) Elevational beam profiles of the steered beam at different wavelengths. (c) Steered angle and FWHM beam width of the corrugated waveguide grating at different wavelengths.

across θ are present and indicate light being emitted at different angles. This scrambling of the far field is due to optical crosstalk and the associated supermodes which have slightly different propagation constants from each other. According to the phase matching condition, these small differences in effective refractive index will cause the light to be emitted at slightly different angles and ultimately scramble the far field pattern. Figure 6(b) shows the far field of an OPA with identical element spacing and 2D PC inserted between each array element. Only a single spot is present, which demonstrates that the PC is successful in blocking the laterally coupled light from the corrugated waveguides, thereby preventing optical crosstalk. The intensity profiles for the θ and ψ (XY plane) directions are shown in Figure 6(c). The lateral beam width is 1.2°, which matches with the theoretical beam width of 1.2° as well. The theoretical value is calculated by considering the far field pattern of a single grating, which forms the steering envelope, and the array factor, which is determined by the number of array elements and their spacing. Using the pattern multiplication theorem, the overall far field of the OPA can be obtained. The longitudinal beam width is 0.4° and also agrees with the theoretical value as well as the results from the single waveguide characterization. The presence of the small sidelobes in the ψ direction is due to non-uniform MMI outputs and random phase errors. This is caused by random fabrication imperfections in the MMI and the waveguide bends which can cause slight differences in the effective index and therefore the phase. This is seen in Figure 6(c) when the phase profile is non-uniform and the side lobe level (SLL), defined as the ratio of the main lobe to the second highest lobe, increases. The experimentally determined SLL is 5dB, and can be reduced to ~10dB with thermo-optic phase tuning as demonstrated by [1-2]. The total device loss is comprised of the input grating coupling efficiency (5.4dB), the total insertion loss of the 4 level cascaded MMIs (3dB), waveguide propagation loss (5dB/cm), and the coupling efficiency of the output grating coupler (3.5dB) for a total device loss of 14.4dB.

IV. Conclusion

In conclusion, we present a grating coupler using corrugated waveguides whose index contrast is lithographically determined and fabricated in a single patterning step. Using wavelength tuning, we achieve 15° of steering with an average beam width of 0.3°, which is the lowest demonstrated to date. In addition, we propose and demonstrate a method of suppressing the optical crosstalk from grating assisted coupling between adjacent corrugated waveguide elements by optically isolating each array element with 2D PC. This crosstalk suppression is demonstrated by the difference in far fields between a 16 element passive array with and without 2D PC. Such a structure can be combined with thermo-optic phase shifters to achieve 2D beam steering with narrow beam widths and low power consumption.

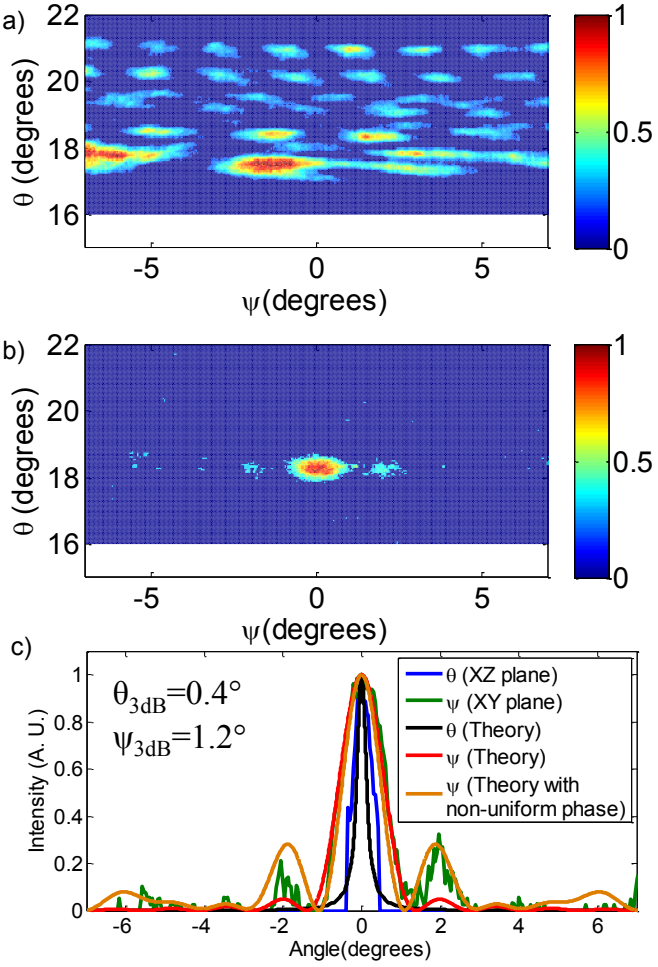

Fig. 6-Far field of the 16 element corrugated waveguide array (a) without and (b) with 2D PC crosstalk suppression. (c) Azimuthal and elevational beam profiles of the far field with 2D PC.

References

[1] K.V. Acoleyen, W. Bogaerts, J. Jágerská, N. L. Thomas, R. Houdré, and R. Baets, Opt. Lett. 34, 1477-1479, 2009.
[2] J. K. Doylend, M. J. R. Heck, J. T. Bovington, J. D. Peters, L. A. Coldren, and J. E. Bowers, Opt. Express 19, 21595-21604, 2011.
[3] X. Chen and H. K. Tsang, Opt. Lett. 36, 796-798, 2011.
[4] X. Xu, H. Subbaraman, J. Covey, D. Kwong, A. Hosseini, and R. T. Chen, Appl. Phys. Lett. 101, 031109, 2012.
[5] S. M. Rytov, Sov. Phys. JETP 2.3 466-475, 1956.
[6] X. Chen, K. Xu, Z. Cheng, C. K. Y. Fung, and H. K. Tsang, Opt. Lett. 37, 3483-3485, 2012.
[7] W. Shi, X. Wang, W. Zhang, H. Yun, C. Lin, L. Chrostowski, and N. A. F. Jaeger, Appl. Phys. Lett. 100, 121118, 2012.
[8] A. Hosseini, D. Kwong, Y. Zhao, Y. S. Chen, and R. T. Chen, IEEE Journal of Selected Topics in Quantum Electronics, vol. 15, no. 5, 1439-1446, 2009.